International Journal of Remote Sensing

An accuracy assessment methodology for the remotely sensed discontinuities: a case study in Andesite Quarry area, Turkey

PLEASE SCROLL DOWN FOR ARTICLE

Taylor & Francis
Taylor & Francis Group

An accuracy assessment methodology for the remotely sensed discontinuities: a case study in Andesite Quarry area, Turkey

A. KOCAL*†, H. S. DUZGUN†‡ and C. KARPUZ†
†METU, Mining Engineering Department, 06531 Ankara, Turkey
‡METU, Geodetic and Geographic Information Technologies, 06531 Ankara, Turkey

The discontinuities play an important role in both the design and development stages of many geotechnical engineering projects. Therefore, semi-automatic detection of discontinuities based on remote sensing will save a considerable amount of time and cost. Accuracy of the semi-automatically detected discontinuities is also as important as the detection process, since the results directly reflect the uncertainty in the geotechnical problem. The current paper presents an accuracy assessment methodology for semi-automatically detected discontinuities from remotely sensed images. Semi-automatic lineament analysis is performed by using high-resolution satellite imagery for identification of rock discontinuities at the Andesite quarry area in Gölbaşı, Ankara, Turkey. A high-resolution data IKONOS Precision Plus with 1 m resolution orthorectified image has been used in the present study. The accuracy assessment methodology is developed based on a comparison of manually extracted lineaments using directional filtering and semi-automatically detected lineaments with LINE module of PCI Geomatica 8.2 and manual intervention. The proposed accuracy assessment methodology considers the accuracy based on location and length of the lineaments. In this respect, it has two dimensions. For the algorithm of the developed methodology, a software called LINECOMP, is coded in Java environment. The LINECOMP is composed of three modules. These are: LINE ADDRESS for identification of pixel addresses of lineaments; which is used for locational accuracy assessment; LINE COMPARE for comparing two lineament maps with respect to lineament pixels, which is used for length-based accuracy; and LINE CLASSIFICATION for classifying the assessed accuracy with respect to the amount of location and length matching. The performance of the proposed accuracy assessment method is also verified by the field studies carried out in the study area.

1. Introduction

Lineaments are any linear features that can be picked out as lines (appearing as such or evident because of contrasts in terrain or ground cover on either side) in aerial or space imagery. The extraction process of linear features from remotely sensed images is called lineament analysis. If they appear geological, these are usually faults, joints or boundaries between stratigraphic formations. Other causes of lineaments include roads and railroads, contrast-emphasized contacts between natural or man-made geographic features (e.g. fence lines). The human eye tends to

---

*Corresponding author. Email: arman@metu.edu.cr

single out both genuine and spurious linear features, so that some of them delineated to be geological may, in fact, be of other origins. (NASA remote sensing tutorial web page)

In mining and geotechnical applications, determination of discontinuities plays an important role both in design and development stages, which require systematic field studies. It is obvious that these field studies are time-and money-consuming operations. Therefore, it is important to minimize the cost and maximize the incomes, and also to take into account the time spent on the field studies. In this respect, detection of discontinuities from satellite images has great potential to reduce the cost of field studies in terms of time and money. In literature there are plenty of studies related to lineament analysis (Vanderbrug 1976, Koopmans 1986, Majumdar and Bhattacharya 1988, Wang and Howarth 1990, Clark and Wilson 1994, Mah *et al.* 1995, Koike *et al.* 1995, Kane *et al.* 1996, Süzen and Toprak 1998, Novak and Soulakellis 2000, Leech *et al.* 2003, Arlegui and Soriano 2003) but these studies do not focus on detecting small-scale line features which are important in mining and geotechnical activities requiring detailed discontinuity maps. In the above-mentioned published studies, medium to low-resolution images have been used covering relatively larger areas than possible mine and geotechnical project sites. Moreover, most of these studies lack an accuracy assessment, in which the reliability of the detected lineaments is determined. There are a few studies on pattern recognition about the lineaments in the literature (Koike *et al.* 1995). Hence, use of lineament detection methods from remote sensing can become efficient in geotechnical and mining applications only if the process is automated with an associated accuracy assessment.

Accuracy assessment determines the quality of the information derived from remotely sensed data (Congalton and Green 1999). Thematic maps obtained from remotely sensed data need to be expressed in terms of degree of correctness (Foody 2002). Accuracy assessment can be both qualitative and quantitative. Qualitative assessments are determined by comparing visually interpreted results of an imagery with what is seen on the ground. On the other hand, quantitative accuracy assessment involves the comparison of quantifiable parameters of a site on a map against reference quantitative parameters of the same site (Congalton and Green 1999).

Accuracy can be categorized into two types: location and classification accuracy. Location accuracy is determined based on matching percentage of the objects that were mapped with the reference. In the classification accuracy, the main aim is to determine the degree of correct and wrongly classified objects.

In remote sensing applications, there are plenty of studies about classification accuracy assessment (Aplin *et al.* 1999, Serra *et al.* 2003, Wang *et al.* 2004). The main procedure of accuracy assessment is to establish the confusion matrix. Among these studies, Serra *et al.* (2003) had studied post-classification change detection with Landsat MSS and TM data. Their study presents a method for reliable post-classification comparisons. The accuracy of the classification is evaluated by confusion matrix. Wang *et al.* (2004) had studied a methodology for integration of object-based and pixel based classification with IKONOS imagery. They have emphasized enhancing the spectral separability among mangrove species by taking the object as the basic spatial unit as opposed to the pixel. Another similar accuracy assessment study of land cover mapping was done by Aplin *et al.* (1999). Confusion

matrices are the key decision-making parameters for evaluating the accuracies of per-pixel classification and per-field classification.

Calculating errors is another perspective of accuracy assessment. Higher accuracies can be obtained by lowering the error percentages. Lopez (2002) had studied the improvement of the elevation accuracy of photogrammetrically derived digital elevation model (DEM) and focused on root mean square error (RMSE) of six DEMs at different places. The RMSEs with three different methods were calculated.

Uncertainties about the locations of data values are routinely addressed in image analysis. Many applications require predictions about multiple-pixel regions (Dungan 2002). Goodchild and Hunter (1997) had developed a simple positional accuracy measure method for linear features. Their study basically deals with comparison of linear features with different buffer zones, and percentage of a line feature within a buffer is given.

As can be seen from the existing literature on accuracy assessment, there exists a common logic whenever a processed map is compared with a reference map. However, accuracy is not assessed based on considering its two components namely classification and location. Furthermore, the approaches in the above studies are for assessing the accuracy based primarily on the data. In the present study, an accuracy assessment methodology is developed based on comparison of lineaments detected manually using directional filtering with that of semi-automatically detected using LINE module of PCI Geomatica 8.2 (2001) with manual intervention. Here, manually detected lineament map serves as reference map to be used for comparison, while the semi-automatically detected lineament map for its accuracy assessment. The methodology is general, which can be applicable to any reference map such as existing structural geology maps, faults maps, etc. The proposed accuracy assessment methodology considers the accuracy based on locations and lengths of the lineaments. In this respect, it considers accuracy assessment of the two components, locations and lengths of the discontinuities at the same time. For the algorithm of the developed methodology, a software called LIMECOMP is coded in a Java environment.

2. Data sources and area of interest

For the implementation of the proposed methodology, multispectral IKONOS-PAN-sharpened image (with 1 m resolution, ortho-rectified) of a mine area, which was captured in October 2002, has been used. The bandwidths of the channels are 0.45–0.53 μm for blue band, 0.52–0.61 μm for green band and 0.64–0.72 μm for red band. The study site, approximately 15 km^2 in area, is located within Gölbaşı town of Ankara province, Turkey (figure 1). The Easting and Northing corners of the image in universal transverse mercator (UTM) projection are given in table 1. There are five main rock units such as tuff, andesite, alluvial, limestone in complex series, ophiolitic dominant complex series (Kadıoglu 2004, personal communiation). The lithological map of the area is given in figure 2. The PAN-sharpened true color composite image of the study area is given in figure 3.

3. Methodology

The proposed methodology has basically two parts: (a) production of lineament maps from remote sensing image based on both manual and semi-automatic
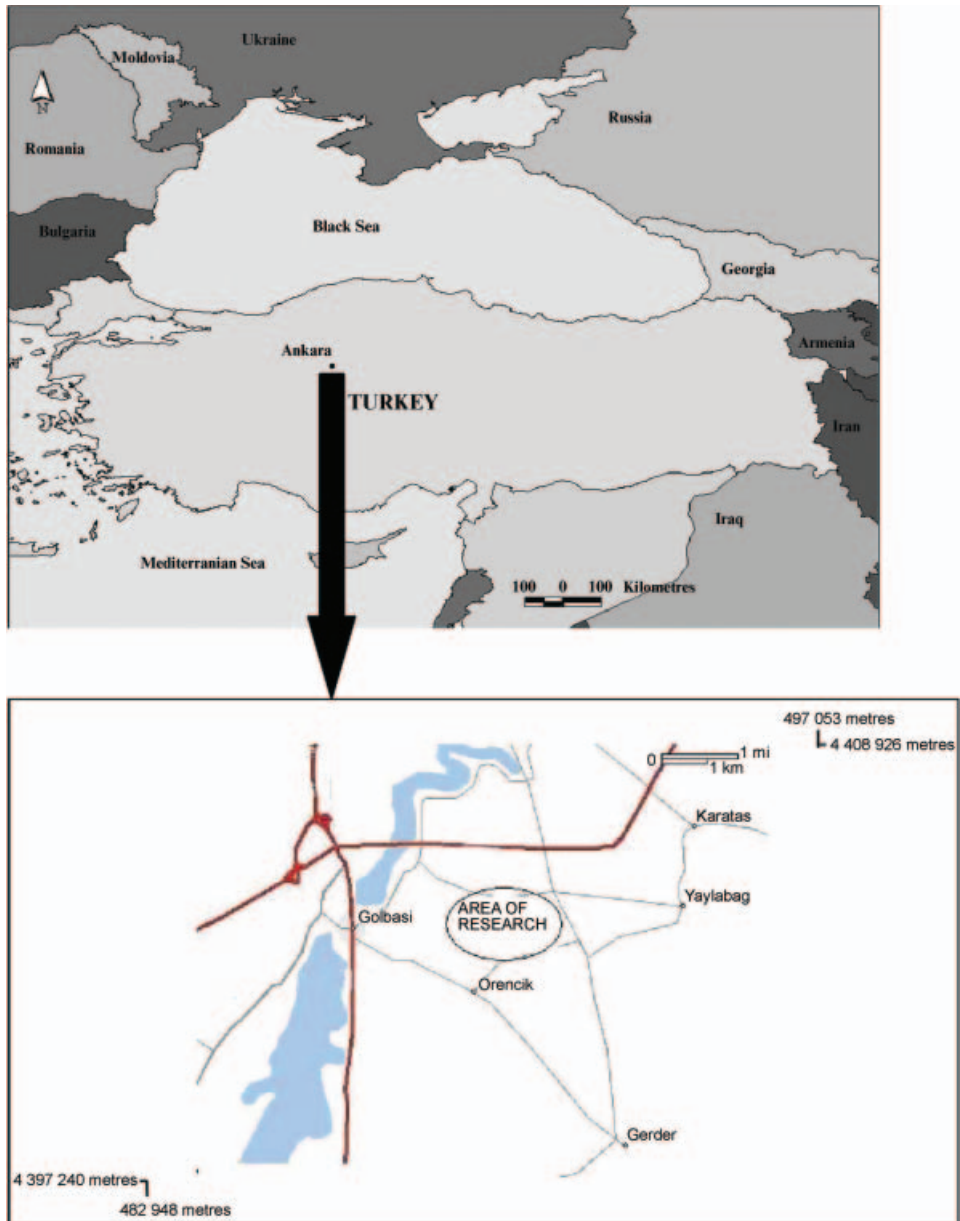
Figure 1.   Location map of the study area.

extraction methods (PART I) and (b) measurement of accuracy assessment's performance based on field studies (PART II). The flowchart of the developed technique is given in figure 4. The steps followed in PART I are as follows:

(1)   produce semi-automatically extracted lineament maps by using PCI Geomatica 8.2 software's LINE option with manual intervention;
(2)   obtain reference lineament map by applying directional filters and then digitizing the identified lineaments. If a structural geology map exists over

Table 1. Corner coordinates of the study area.

Corner	Easting	Northing
North-west	488234	4405640
North-east	492339	4405640
South-east	492339	4401954
South-west	488234	4401954

the study region, it can be used as a reference map and hence step 2 can be omitted;

(3) prepare Rose diagrams of the lineaments obtained by manual (reference) and semi-automatic extraction processes to compare the directional accuracy of the detected lines;

(4) apply LINECOMP algorithm to assess the accuracy of semi-automatic lineament extraction process.

In PART II, the basic aim is to support the developed accuracy assessment methodology based on field observations. The steps of PART II are as follows.

(1) Verify the results of PART I by visual inspection in the field.

(2) Process the images taken from the excavated rock faces and produce the lineament maps.
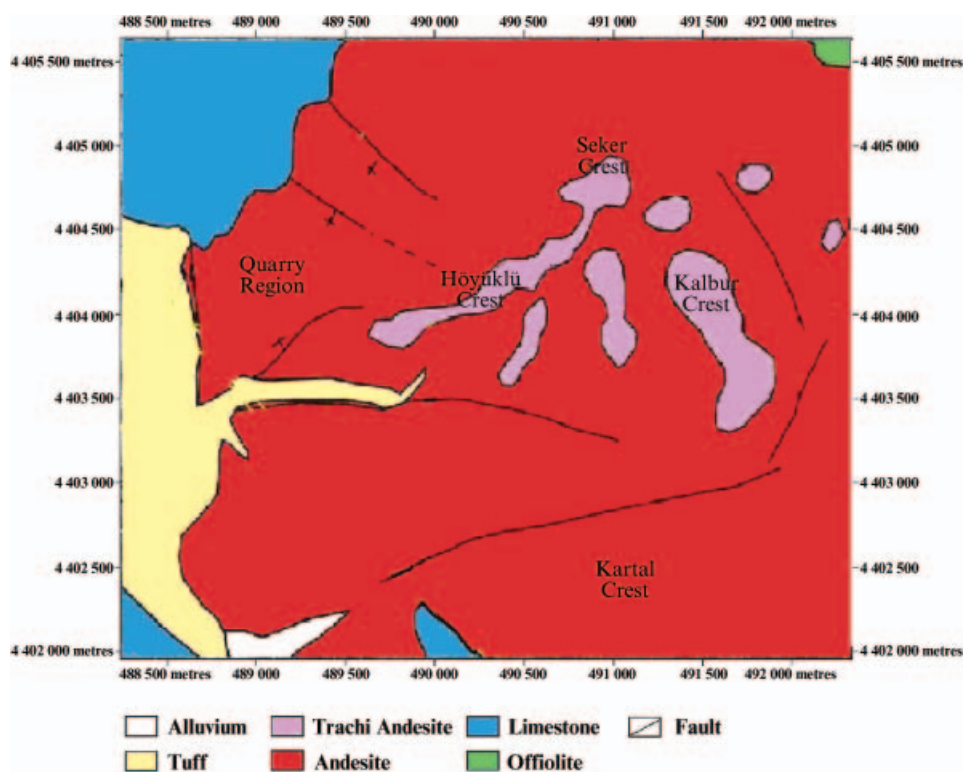
Figure 2. Lithological map of the study area (Kadıoğlu 2004, personal communication).

A. Kocal et al.
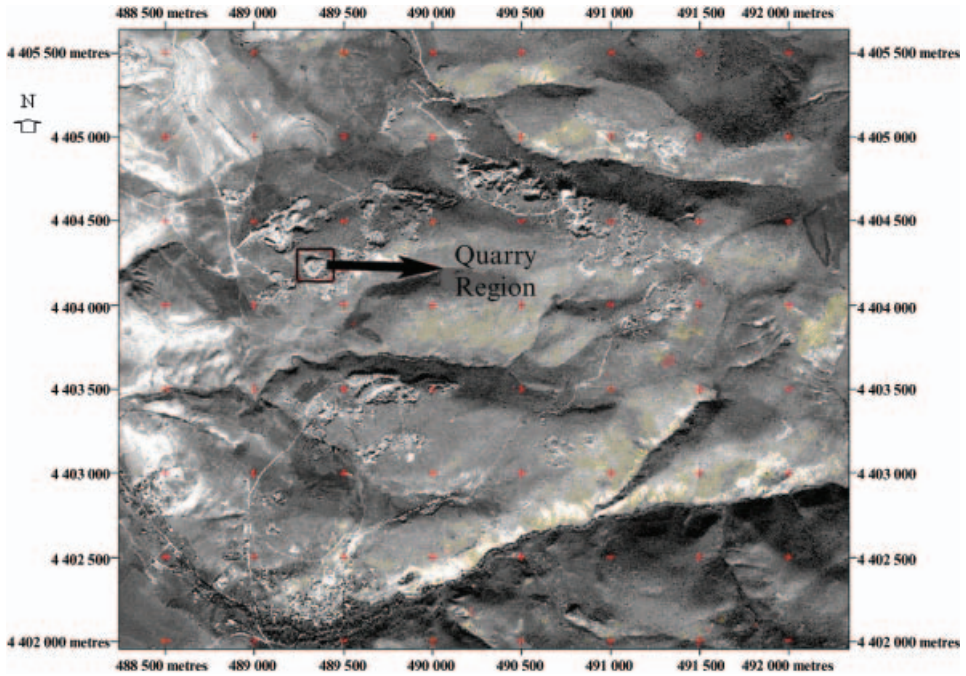
Figure 3.   Pansharpened true colour composite ımage of the study area.

(3) Compare the slope face lineaments and surface lineaments. This comparison
     is performed owing to the fact that the lineaments obtained from the
     remotely sensed images are the traces of rock discontinuities, while the
     lineaments obtained from the excavated rock faces constitute the extent of
     rock discontinuities under the ground. For this reason, it is possible to
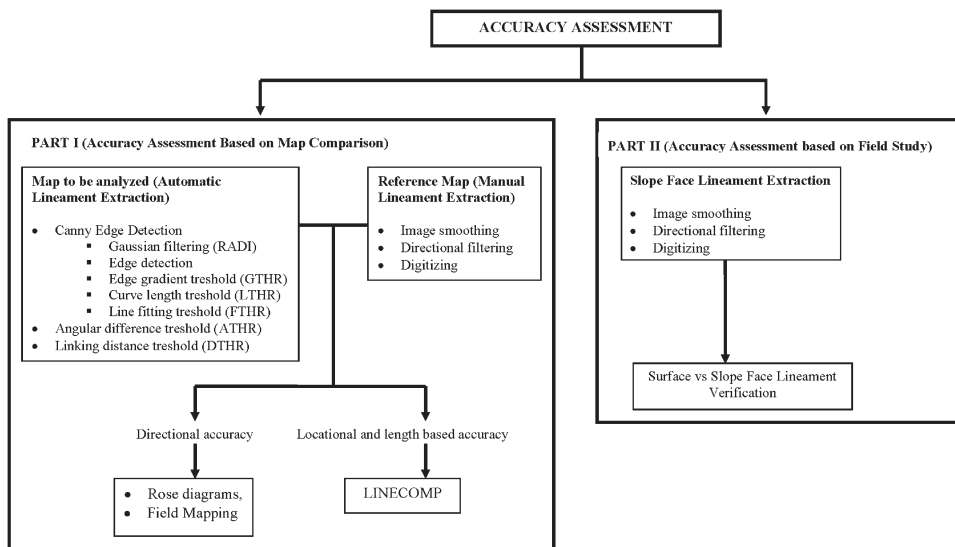
Figure 4.   Flowchart for the developed technique.

extract information about the dip and strike of the discontinuities from excavated faces, where it is possible to relate the strike with the orientation of discontinuity traces found from remotely sensed images.

3.1 *Production of lineament maps*

The map of semi-automatically detected lineaments is produced by using LINE option of PCI Geomatica 8.2 and with some manual intervention. LINE extracts linear features from an image and records the polylines in a vector segment, and it has the following global parameters:

RADI	Radius of filter in pixels
GTHR	Threshold for edge gradient
LTHR	Threshold for curve length
FTHR	Threshold for line fitting error
ATHR	Threshold for angular difference
DTHR	Threshold for linking distance

The algorithm of LINE consists of three stages: edge detection, thresholding and curve extraction. In the first stage, the Canny edge detection algorithm is applied to produce an edge strength image where the input image is filtered with a Gaussian function whose radius is given by the RADI parameter. In the second stage, the edge strength image is thresholded to obtain a binary image by the GTHR parameter. In the third stage, curves are extracted from the binary edge image. This step consists of several substeps. Initially, a thinning algorithm is applied to the binary edge image to produce pixel-wide skeleton curves. Next, a sequence of pixels for each curve is extracted from the image. Any curve with the number of pixels less than LTHR is discarded. The extracted curve is then converted to vector form by fitting piecewise line segments to it. The resulting polyline is an approximation to the original curve where the maximum fitting error (distance between the two) is specified by the FTHR parameter. Finally, the algorithm links pairs of polylines that satisfy the following criteria. (PCI Geomatica 8.2 Online User's Manual, 2001)

(a) end segments of the two polylines face each other and have similar orientation (the angle between the two segments is less than the parameter ATHR);

(b) end segments are close to each other (the distance between the end points is less than the parameter DTHR).

The threshold values for six parameters were defined by trial and error approach. The different values of parameters are tried and then the total number of lineaments obtained from each set of parameters was evaluated. The parameters with total length and number of semi-automatically extracted lineaments together with the corresponding parameters are given in table 2.

The second step in the proposed accuracy assessment methodology is the production of a reference map. In this case, as no structural geology map is available, a reference map has been prepared by manual extraction. The image is first smoothed with an average low pass filter. When directional filtering is applied to the image the lineaments show up in light colour, which are surrounded by dark colored pixels. Initially, the image that was filtered in N–S direction is digitized on a scale of 1:1500. Following that, the lineaments in the E–W filtered image were

Table 2. Parameters, total length and number of lineaments formed by semi-automatic extraction.

LINE ID	Parameters					Length (m)	Number
	RADI	GTHR	LTHR	FTHR	ATHR		
1	5	20	10	2	20	112195	2883
2	5	20	20	2	20	122827	3056
3	5	20	15	2	20	165649	5404
4	5	20	25	2	20	89641	1901
5	5	30	15	2	20	104321	3312
6	5	30	20	2	20	74361	1887
7	5	40	15	2	20	69366	2265
8	12	40	25	2	20	117572	2368
9	12	20	25	3	20	210940	4418
10	12	20	25	3	30	252699	4846
11	12	20	25	3	40	298381	5468
12	12	30	20	3	30	245697	5235
13	12	30	30	3	20	135713	2415
14	12	30	25	3	20	172840	3520
15	12	30	20	3	20	225425	5213
16	12	40	25	3	20	139668	2776
17	12	50	25	3	20	115504	2256
18	12	40	20	3	20	181198	4101
19	12	50	20	3	20	147397	3271
20	12	40	15	3	20	235470	5986
21	12	50	15	3	20	189130	4692
22	12	60	15	3	20	153974	3752
23	12	60	20	3	20	120410	2589
24	12	60	25	3	20	95778	1833
25	12	100	15	3	20	78245	1807
26	7	20	25	2	20	140652	2496
27	7	30	20	2	20	135568	2736
28	9	30	20	2	20	145870	3410
29	9	30	25	2	20	150876	3258

added to the previously extracted lineaments in the N–S filtered image. Similarly the lineaments in the NW–SE and NESW directions were added to the vector layer respectively, and the lineament map of the study area was prepared. In all, 3065 lineaments with about 130 040 m total length, have been manually extracted and given in figure 5. The raw image shown in figure 3 also contains agricultural field boundaries, houses in the villages and roads. These are all excluded while digitizing. Hence, in the manually produced lineament map, a boundary of the area of interest was formed. The automatically extracted lineaments were overlaid with the reference data and the lineaments delineated by automatic extraction process occurring outside the boundary area were deleted. Deleting the vectors that correspond to the non-geological features will increase accuracy and enhance the applicability of the methodology in terms of detecting the discontinuities. As there is manual intervention in the automatically extracted lineament maps after LINE option, the method for lineament extraction is called as semi-automatic.

The total number of lineaments in manually extracted lineament map and that in semi-automatically extracted lineament maps are computed with different parameters of LINE options. Then the seven lineament maps which have total number of lineament values closer to the number of lineaments in manually extracted lineament map are selected. These seven maps have total number of lineaments within 10% of
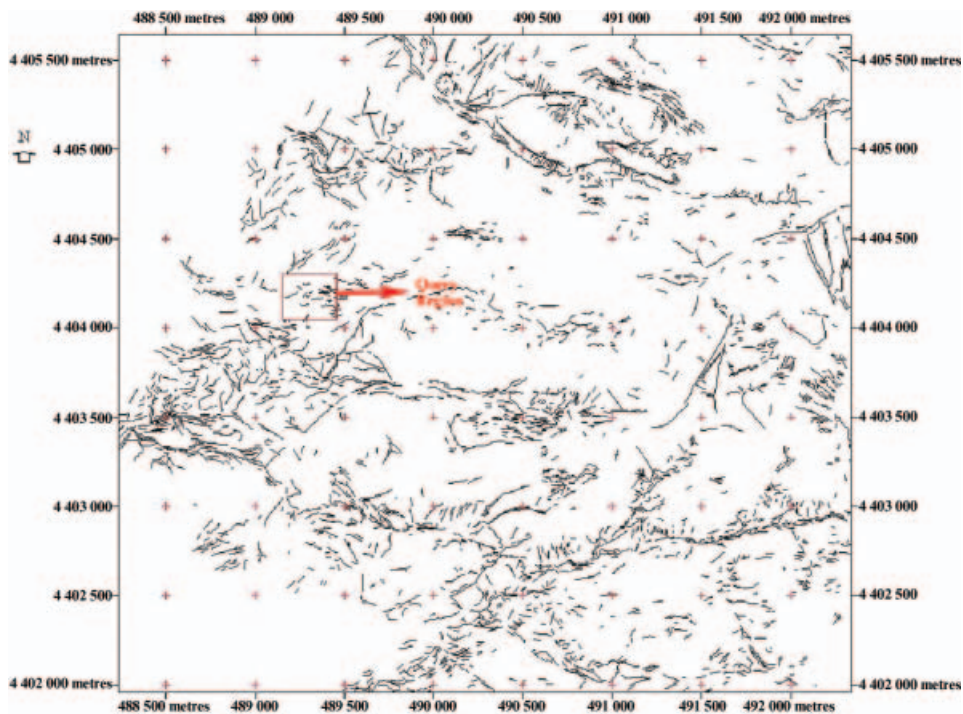
Figure 5.   Manually extracted lineament map of the area of interest.
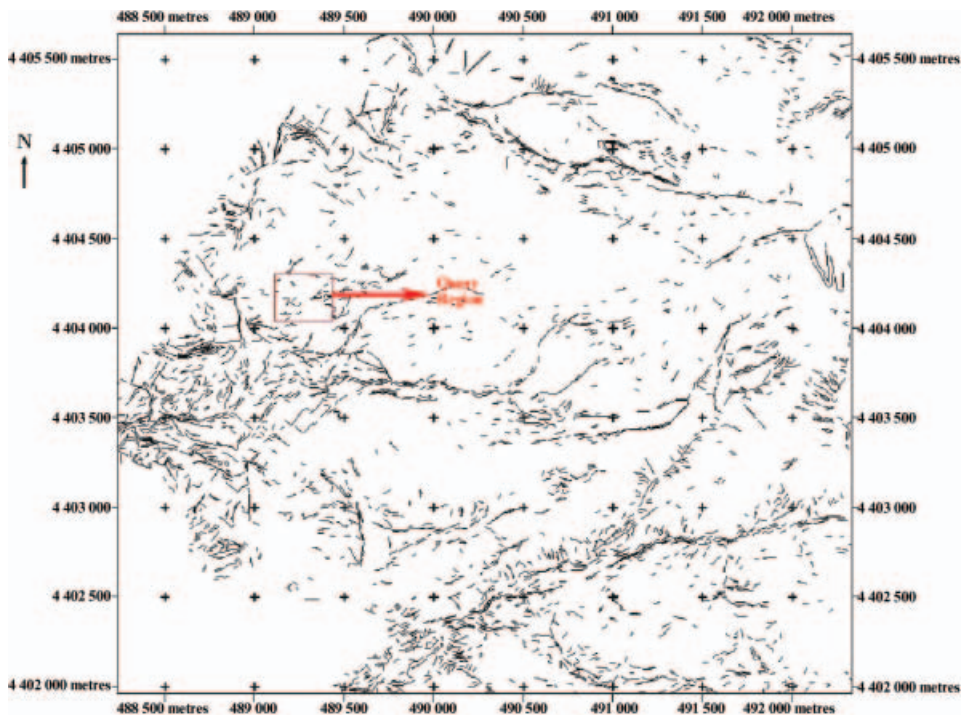

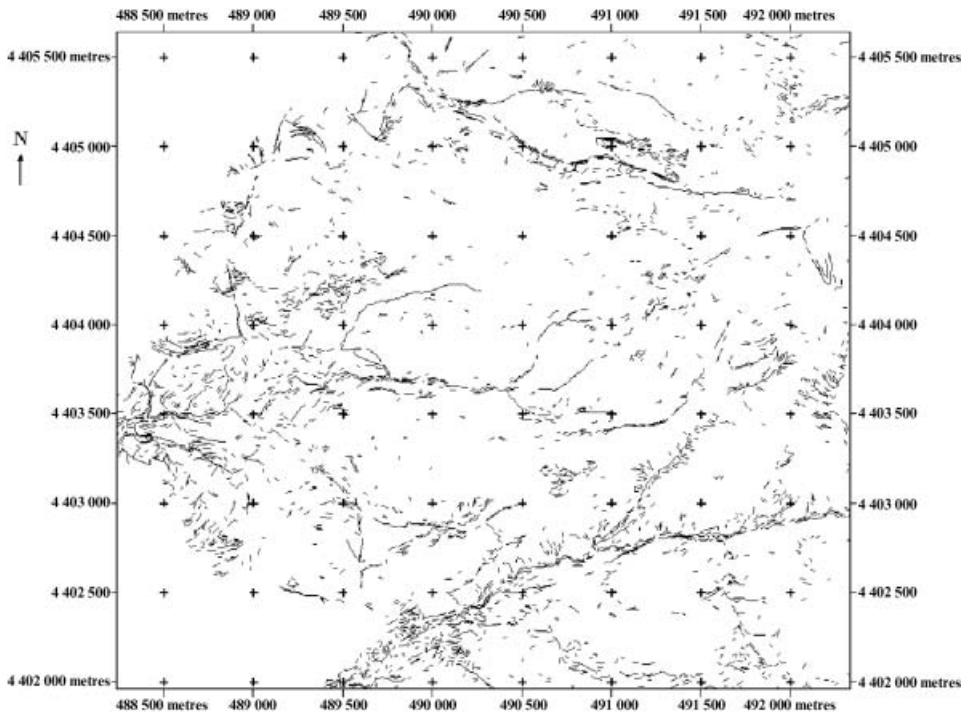Figure 6.   The semi-automatically extracted lineament map LINE 2.

Figure 7. The semi-automatically extracted lineament map LINE 5.

the total lineaments detected in manually extracted maps. The typical selected maps satisfying above criteria are given in figures 6 and 7. For example, there are 3065 lineaments in manually extracted map. The lineament maps containing lineaments between 2758 and 3372 are selected for further analysis. The lineament maps are selected from table 2 and the selections are listed in table 3.

3.2 Directional accuracy assessment (Rose diagrams)

The applicability of the semi-automatic lineament extraction technique for delineating lineaments from remote sensing image needs to be verified. Field observations and the measurements is the first verification method. The second one

Table 3. Number of lineaments classified according to matching pixels with tolerance value=1.

LINE ID	Number of lineaments	Number of non-matching lineaments	Number of perfectly matching lineaments	Number of longer lineaments	Number of shorter lineaments	Percent of non-matching lineaments
1	2883	1630	6	1010	237	56, 54
2	3056	1703	11	1071	271	55, 73
5	3312	2093	10	1056	150	63, 19
16	2776	1873	2	855	46	67, 47
19	3271	2266	2	936	67	69, 28
27	2736	1720	7	920	89	62, 87
29	3258	2009	9	1083	157	61, 66

is the comparison of manually digitized discontinuity map with semi-automatically extracted lineament map. The first method was utilized to check the directional accuracy of the lineament maps. For this purpose, Rose diagrams of semi-automatically and manually extracted lineament maps were prepared and compared with each other. This comparison is also made by using the field measurements of Karpuz (1982).

For the Rose diagram applications, the 'node to node' method was used in order to evaluate a lineament independently from the line segments forming it. This method uses the direction of a simple line segment that connects the endpoints (nodes) of the line element. Node to Node method gives satisfactory results because the extracted lineaments do not have a 'fish hook' or 'horseshoe' shape. One example of Rose diagrams for the selected semi-automatically extracted lineaments is shown in figure 8, while that of the manually extracted lineaments is shown in figure 9. Rose diagrams show the similarities in major discontinuity orientations. Both the manually prepared reference lineament map and the semi-automatically extracted lineament maps have the major orientation E–W. In addition, a site investigation is necessary for more accurate analysis. The field discontinuity measurements carried out at a quarry, yielded two major sets with strikes N80° E, N70° W and a minor set of N20° E. The pole distribution of the discontinuities observed in the field is given in figure 10.

3.3 *Developed accuracy assessment method (LINECOMP algorithm)*

In geotechnical and mining applications, not only the orientations of the discontinuities but also the length and location of them are important. For this reason, a simple image comparison algorithm is not sufficient to determine length and locational accuracy. The method introduced here detects the length and locational accuracy of the discontinuities and also evaluates the matching levels of
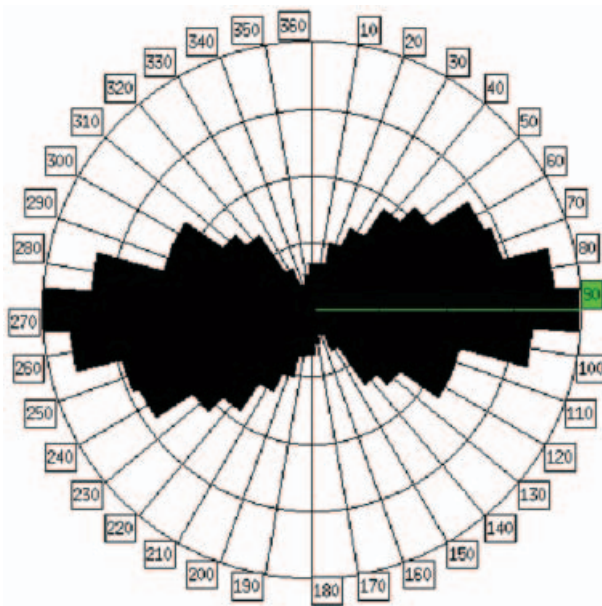

Figure 8.   Rose diagram of LINE 2.
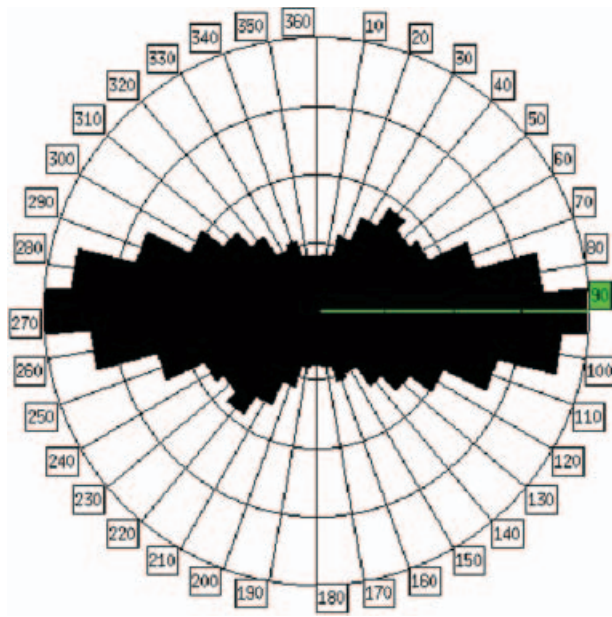
Figure 9.   Rose diagram of manually extracted lineaments.

the manually and semi-automatically extracted lineament maps. In the present study, 10% discrepancy between the numbers of the manually and semi-automatically extracted lineaments was considered to be reasonable. The resultant lineament maps of LINE module were represented in vector format and for the quantitative evaluation of the accuracy, the maps were converted into raster format. Accordingly, each pixel forming the lineament is represented by a digital number.

The vector layers were rasterized, and for the manually extracted map, digital number of 10 is assigned to the vectors. The result is a raster map with pixel value 10 for lineaments and 0 for the others. Similarly for the semi-automatically extracted

Figure 10.   Pole distribution of discontinuity sets observed in the field.

vector maps, a raster map with pixel value 10 for the lineaments and 0 for the others was prepared.

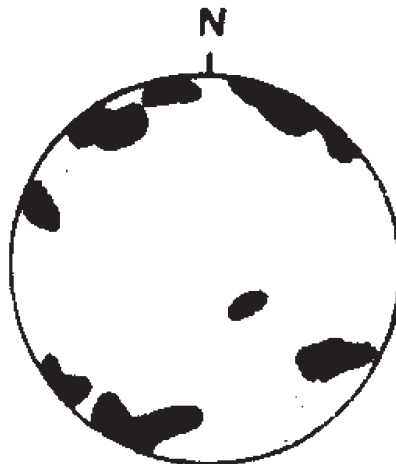An accuracy assessment based on comparing the numbers found by the two different methods is not sufficient. It is necessary to compare them with respect to their location. The location of a lineament was defined by the pixel address. The raster maps obtained from vector rasterization have a size of 3685×4104 (row $\times$ column) pixels. Every lineament pixel has an address $i \times j$, i for row number and j for column number. As a result, after vector rasterization, a matrix was formed with a value 10 representing the lineaments and the rest with a value 0. The two

I

INPUT: ASCII text format of rasterized map

LINE ADDRESS

OUTPUT: Lineament Ids with pixel addresses

II

INPUT: Output of LINE ADDRESS

LINE COMPARE

OUTPUT: Lineament ID of semi-automatically extracted lineament map, matching lineament ID in manually extracted lineament map, matching pixel numbers and matching percentage

Tolerance value

III

INPUT: Output of LINE COMPARE

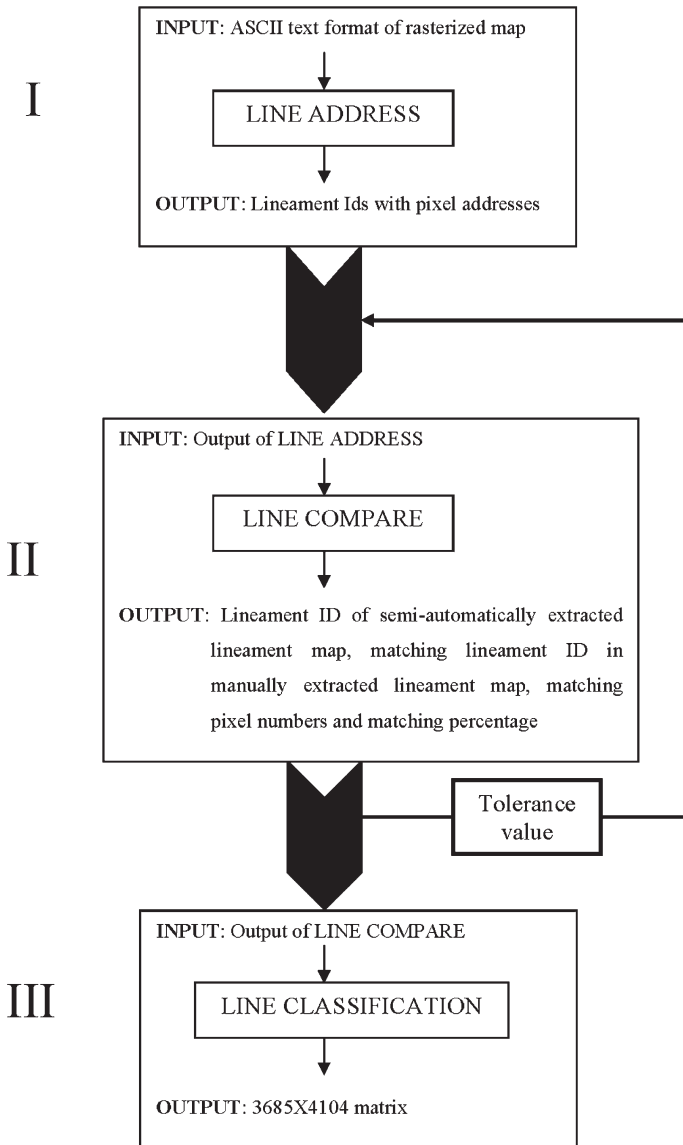LINE CLASSIFICATION

OUTPUT: 3685X4104 matrix

Figure 11.   Algorithm of the developed software LINECOMP.

maps were then compared by using a developed software called LINECOMP coded in Java environment. LINECOMP has three modules. These are: LINE ADDRESS for identification of pixel addresses of lineaments, which is used for locational accuracy assessment, LINE COMPARE for comparing two lineament maps with respect to their lengths, and LINE CLASSIFICATION for classifying the assessed accuracy with respect to their location and length. The algorithm of LINECOMP is given in figure 11.

The algorithm of the LINE ADDRESS is as follows:

(a) scan the lineament map in raster format;
(b) catch the first pixel with value 10 and note the address as Lineament $1=[i_1, j_1]$;
(c) search the neighbourhood of that pixel and find the other 10 and add that pixel's address to Lineament 1 as Lineament $1=[i_1, j_1],[i_2, j_2]$
(d) repeat steps 2 and 3 until there is no neighbourhood pixel with value 10.
(e) continue to scan the image from the first pixel for the other lineaments. Do not record one lineament more than once.
(f) record the number of lineaments and pixel addresses of each lineament.

For the case of intersecting two or more lineaments, LINE ADDRESS detects these lineaments as one lineament. Simple illustration of this case with two intersecting lineaments is given in figure 12. The number 10 represents the lineament pixels. After combining the two intersecting lineaments, the pixel addresses of the lineament is recorded.

The second step of the LINECOMP compares the two lineament maps. For this purpose, the output of LINE ADDRESS is used as input of LINE COMPARE. The semi-automatically extracted lineament maps are compared with the manually extracted lineament map with the second module of LINE COMPARE. After the pixel addresses are determined, the output gives the percent matching of lineaments. The algorithm of the LINE COMPARE part is as follows.

(1) The first vector in the semi-automatically extracted lineament map is compared with all of the lineaments in the reference map and the one that has maximum number of matching pixels is selected.
(2) The matching lineament ID in semi-automatically extracted lineament map, number of pixels, matching lineament ID in manually extracted lineament map, matching pixel numbers and percent of matching are recorded.

j \ i	1	2	3	4	5	6	7	8
1	0	0	**10**	0	0	0	**10**	0
2	0	0	0	**10**	0	**10**	0	0
3	0	0	0	0	**10**	0	0	0
4	0	0	0	**10**	0	**10**	0	0
5	0	0	**10**	0	0	0	**10**	0
6	0	0	0	0	0	0	0	0

OUTPUT

Lineament_1
[1,3][2,4][3,5][4,4][5,3][2,6]
[1,7][4,6][5,7]

Figure 12. Simple illustration of intersecting lineaments in LINE ADDRESS.

Table 4. Sample output of LINE COMPARE.

Lineament ID	Number of pixels	Lineament ID in the reference	Number of matching pixels	Matching percentage
1	30	2	10	33
2	100	4	70	70
3	5	8	2	40
4	6	9	4	67

(3) The same procedure is applied until the last lineament in the semi-automatically extracted lineament map is compared.

A sample output of LINE COMPARE is given in table 4.

If a lineament in reference map matches with more than one lineament in the semi-automatically extracted lineament map, it is compared with both of the lineaments. Simple illustration of this case is given in figure 13.

For eliminating the small pixel address differences of the lineaments, a tolerance value option is available in the program. The user-defined tolerance value defines a pixel based buffer level for each lineament in the reference map. The comparison is then made with the defined tolerance value. The simple illustration of this algorithm is shown in figure 14 as an 8×6 matrix. The value 10 indicates the pixel containing lineament. The 10 values that are bold indicate the buffer pixels when the tolerance value is equal to 1. Thus, the values 10 in the matrix are compared with the values 10 in the reference matrix. The output of this example is 100% matching. As this comparison is pixel based, each pixel represents the spatial resolution of the image. In this study, tolerance value equal to 1 means 1 metre buffer level is used in comparison. Therefore the criteria for selecting a tolerance value are related with the

j / i	1	2	3	4	5	6	7	8
1	0	0	10	0	0	0	0	0
2	0	0	0	10	0	0	0	0
3	0	0	0	0	10	0	0	0
4	0	0	0	0	0	10	0	0
5	0	0	0	0	0	0	10	0
6	0	0	0	0	0	0	0	10

j / i	1	2	3	4	5	6	7	8
1	0	0	10	0	0	0	0	0
2	0	0	0	10	0	0	0	0
3	0	0	0	0	10	0	0	0
4	0	0	0	0	0	0	0	0
5	0	0	0	0	0	0	10	0
6	0	0	0	0	0	0	0	10

Reference Matrix   Matrix to be Compared

OUTPUT

Lineament Id	Number of pixels	Lineament Id in the reference	Number of matching pixels	Matching precentage
1	3	1	3	100
2	2	1	2	100

Figure 13.   Illustration of matching of divided lineaments.

j / i	1	2	3	4	5	6	7	8
1	0	0	0	10	10	10	10	0
2	0	0	0	10	10	10	10	0
3	0	0	0	10	10	10	10	10
4	0	0	0	0	10	10	10	10
5	0	0	0	0	0	10	10	10
6	0	0	0	0	0	10	10	10

Reference matrix

j / i	1	2	3	4	5	6	7	8
1	0	0	0	0	0	0	0	0
2	0	0	0	10	0	0	0	0
3	0	0	0	0	10	0	0	0
4	0	0	0	0	0	10	0	0
5	0	0	0	0	0	10	0	0
6	0	0	0	0	0	0	0	0

Matrix to be compared

Figure 14. Sample illustration of tolerance value in LINE COMPARE Algorithm.

degree of precision demanded. Higher is the selection of tolerance value, lesser is the precision.

The next step after the determination of the matching percentages process was to recognize the matching pixels in the image. For this purpose, the output of the LINE COMPARE was used to classify the percentages by LINE CLASSIFICATION. The algorithm of LINE CLASSIFICATION is as follows:

(1) Take the output of LINE COMPARE and examine the matching percentage of the first lineament,
(2) Classify the first lineament as:

    (a) non-matching lineament if matching percentage=0, with a cell value # 1;
    (b) perfectly matching lineament if matching percentage=100, with a cell value # 2;
    (c) longer lineament if matching percentage >0 and <100, with a cell value # 3;
    (d) shorter lineament if matching percentage >100, with a cell value # 4;
    (e) non-lineament for the rest;
    (f) form the output matrix by taking the pixel addresses of each lineament from output of LINE ADDRESS.

After the classification of the results into four (non-matching, perfectly matching, longer and shorter lineaments), the matrices were again constructed according to the classification. The non-lineament pixels are valued as 0 and the 3685×4104 matrix is formed in Java. It is then imported as a raster image with cell size of 1 m. After the raster image is formed, it is important to recognize the classified pixels in the image. For this reason, different colours are assigned to different pixel values. The assigned colours for pixel values and a sample classified image are given in figures 15 and 16 respectively.

In order to determine the most suitable parameters of PCI Geomatica's LINE option, the previously selected seven semi-automatically extracted lineament maps (LINE 1, LINE 2, LINE 5, LINE 16, LINE 19, LINE 27 and LINE 29) were compared with manually extracted lineament map with LINE COMPARE with tolerance value 1. The results of the comparison of the semi-automatically and
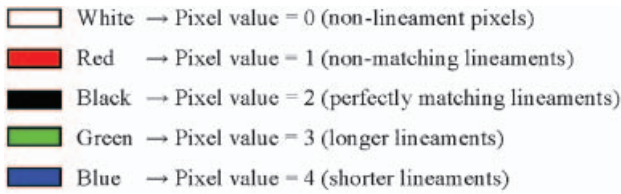
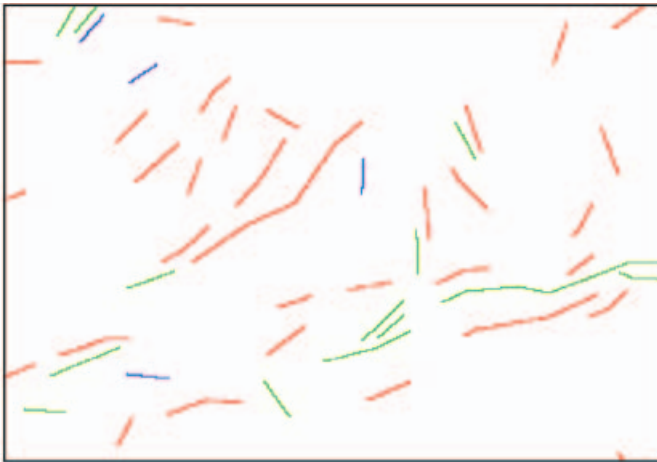Figure 15. Assigned colours for pixel values.

Figure 16. Sample classified map.

manually extracted lineament maps with a tolerance value equal to 1 are given in table 3.

Some typical classified images of LINECOMP obtained in a selected zone are presented in figures 17 to 19. Figure 17 representing map with tolerance value 1 shows that the non-matching lineaments (red pixels) and lineaments that are longer in semi-automatic extraction (green pixels) are dominant. Figure 18 shows the results of the
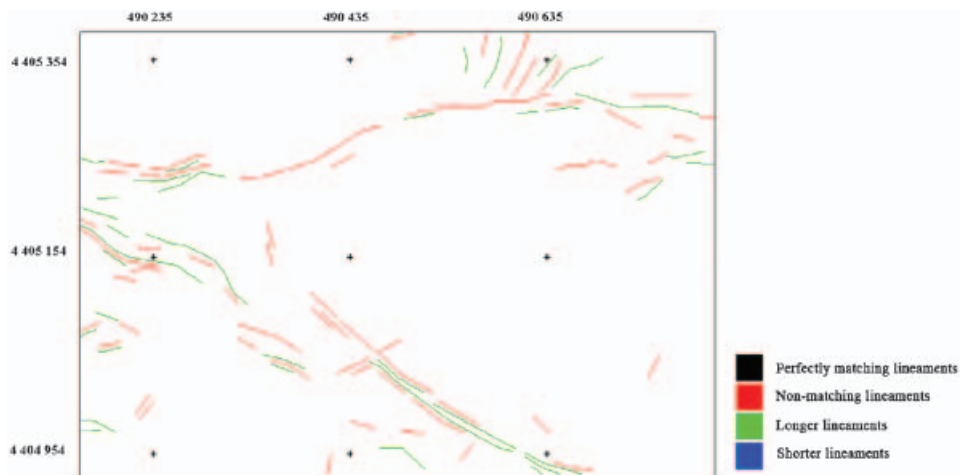

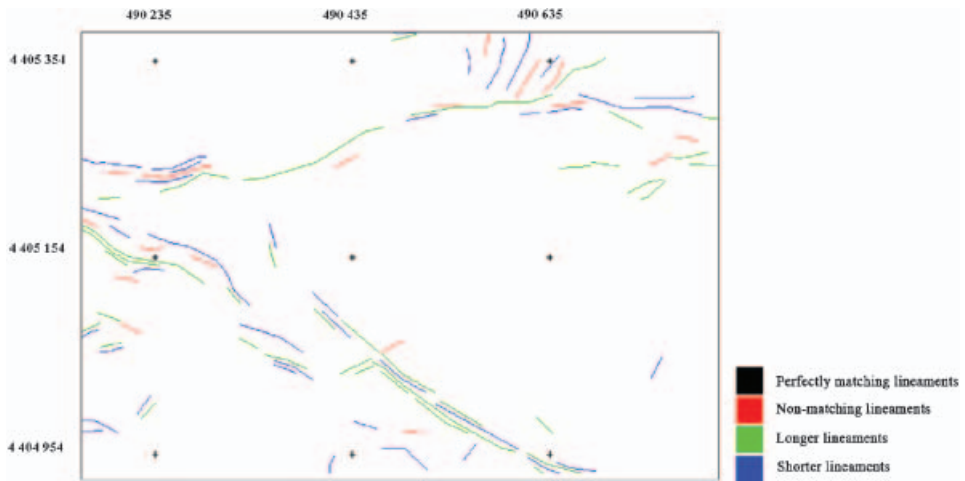Figure 17. Classified image of LINE 2 with tolerance value=1.

Figure 18.   Classified image of LINE 2 with tolerance value=4.

tolerance value 4. The red pixels are turned into green. It means semi-automatically extracted non-matching lineaments started to match and they are greater in length. Figure 19 shows that shorter lineaments are getting more dominant in the classified images as the tolerance value is increased to 7. Green pixels are turned into blue. That is, the semi-automatically extracted lineaments become shorter than manually extracted lineaments because of the reason that the number of buffer lineament pixels increase with the increasing tolerance value.

Besides the general directional behaviour, the analytical comparison of the methodology gives more reliable results compared to that by the conventional method. First impression about the results can be obtained from the percentage of the non-matching pixels illustrated in red colour in the maps. As the number of the lineaments increases, the percentage of non-matching pixels also increases because the difference in number of lineaments increases. Tolerance value is another factor that affects the accuracy of the matching of the lineaments. As the tolerance value
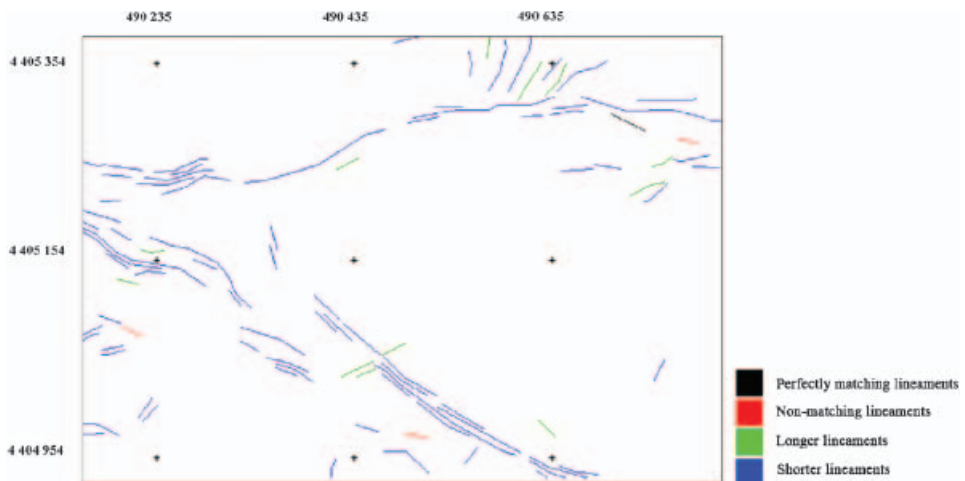

Figure 19.   Classified image of LINE 2 with tolerance value=7.

increases, the percentage of perfectly matching pixels, illustrated in black colour, also increases. On the other hand, increasing tolerance value decreases the sensitivity of the analysis. With the increase in tolerance value, the red (non-matching lineament pixels) and green (longer lineament pixels) pixels change to blue (shorter lineament pixels) pixels. When the tolerance value is increased to 4, besides the decreasing number of both red and green pixels, there is also a decrease in the number of black pixels (perfectly matching lineament pixels) with a consequent decrease in the number of non-matching lineaments. The reason for decreasing of the black pixels is the length change of the lineaments in the reference map. As the tolerance value is increased, the lineaments in the reference map become longer. Therefore, the lineaments in the manually extracted map become shorter. Finally, at the tolerance value of 7, almost all the green lineaments turn into blue. The number of red lineaments continues to decrease.

3.4 *Field study*

Field studies were carried out to verify the lineament orientation of the discontinuities determined from the satellite image. For this determination, a quarry face in the studied area was utilized in two different ways (figures 3, 5 and 6). First, the distinguished discontinuities were measured by a conventional way using a compass, (dip directions and their strikes shown in figure 20). Second, the quarry face in the area was photographed with a 2.0 megapixel digital camera from coordinates of 4 404 212 N – 489 200 E. The lineament detection process of the digital photo was performed by manual extraction of the lineaments from the image after directional filtering. Face discontinuity sets are given in figure 21. The determined lineaments from the quarry face (by both conventional and photo techniques) were coincided with the lineaments determined from satellite image, in one case which corresponds to a minor discontinuity set.

4. Results and discussions

From the analyses carried out at the andesite quarry area of the Gölbaşı District of Ankara, Turkey, a tolerance value of 4 is recommended for matching the manually extracted lineaments with semi-automatically extracted lineaments. As a summary:

(1) From tolerance value # 0 (one-to-one matching) to # 4, the absolute changes in the number of non-matching lineaments decreases considerably.
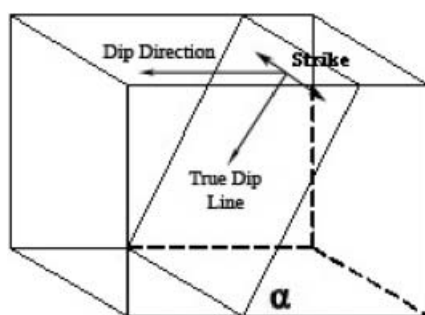

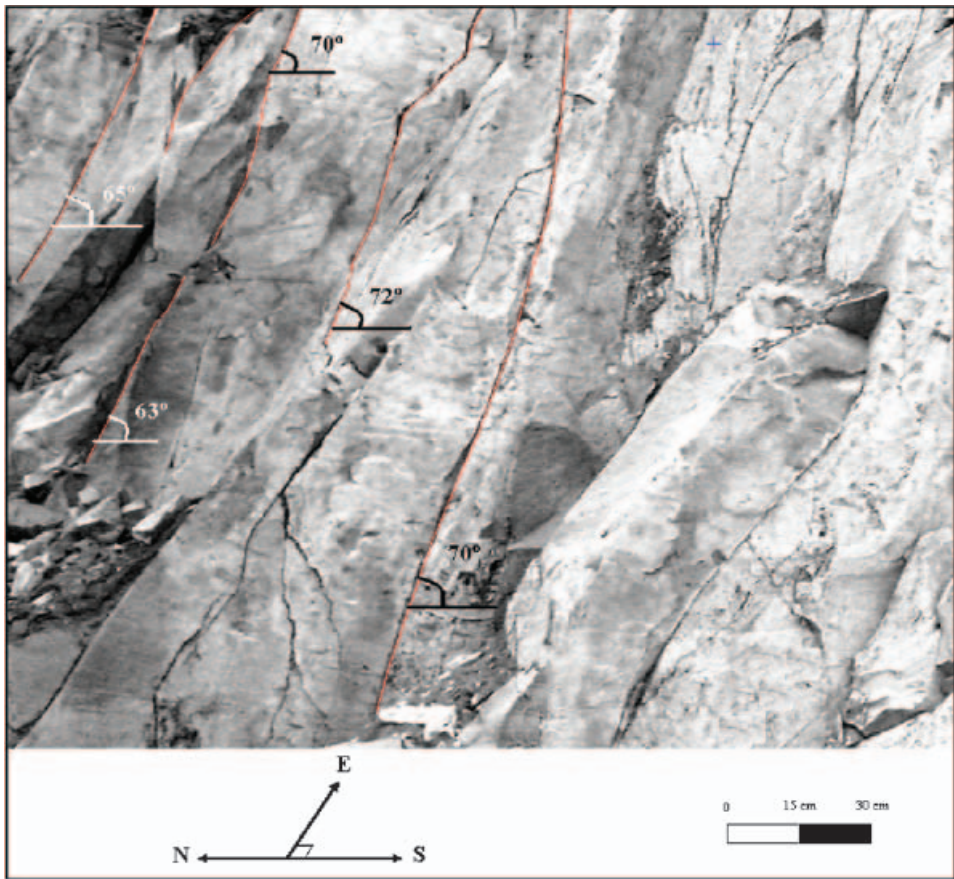Figure 20.   Sketch of dip direction versus strike.

A. Kocal et al.

Figure 21.   Lineaments of the quarry face.

(2) Tolerance values higher than 4 show a decrease in the number of perfectly matching lineaments with an increase in shorter lineaments and the absolute change in non-matching lineaments decreases gradually. Sensitivity of the application also decreases accordingly.

Table 5. Matching percentages of LINE 2 with different tolerance values.

Tolerance value	Number of non-matching lineaments	Number of perfectly matching lineaments	Number of longer lineaments	Number of shorter lineaments	Percent of non-matching lineaments
0	2179	0	0	877	71, 30
1	1703	11	1071	271	55, 73
2	1448	14	1202	392	47, 21
3	1257	11	850	938	40, 41
4	1104	11	703	1238	36, 13
5	1004	7	579	1466	32, 49
6	918	5	490	1643	30, 04
7	872	3	423	1758	28, 53

(3) With further increase in tolerance values, green lineaments (longer) turn into blue (shorter) and red lineaments (non-matching lineaments) continue to decrease slowly.

It can thus be concluded that the lineament maps can be matched effectively with tolerance value of 4 (table 5).

The main results obtained from this study are as follows:

(1) Besides a quantitative accuracy assessment, a location-direction-length based accuracy assessment methodology has been developed and a program called LINECOMP has been coded in Java environment.

(2) The parameters for using automatic lineament extraction for discontinuity mapping has been established. For the accuracy assessment procedure, the most applicable parameters of PCI Geomatica 8.2 for this study have been identified as follows

- RADI=5
- GTHR=20
- LTHR=20
- FTHR=2
- ATHR=20
- DTHR=1

(3) The directional analysis of the semi-automatically extracted lineament maps has been carried out using manually extracted lineaments and previous studies in this research area as reference. The results verify the similarity in the directional behaviour of the lineaments.

(4) With the field studies, face discontinuities are found to be related with the surface lineaments.

5. Conclusions and recommendations

The accuracy assessment of lineament maps requires the accuracy estimation of three components: length, location and orientation. In the present study, the locational and length accuracies have been detected based on a developed algorithm called LINECOMP, while the directional accuracy is assessed using field studies and Rose diagrams. Here, manually extracted linemament map has been used as the reference map, since there was no structural geology map available over the study region. However, the methodology will be applicable to any reference map, as well.

The developed methodology also serves as a systematic approach in accuracy assessment, where uncertainties in the use of remote sensing applications to geotechnical and mining engineering can easily be assessed. It especially helps mining, marble quarrying and geotechnical planning studies.

References

APLIN, P., ATKINSON, P.M. and CURRAN, P.J., 1999, Fine spatial resolution simulated satellite sensor imagery for land cover mapping in the United Kingdom. *Remote Sensing of Environment*, **62**, pp. 206–216.

ARLEGUI, L.E. and SORIANO, M.A., 2003, An example of a comparison between Thematic Mapper and radar images in the central Ebro basin. *International Journal of Remote Sensing*, **24**, pp. 457–474.

CLARK, C.D. and WILSON, C., 1994, Spatial analysis of lineaments. *Computers and Geosciences*, **20**, pp. 1237–1258.

CONGALTON, R.G. and GREEN, K., 1999, Assessing the accuracy of remotely sensed data: principles and practices (Boca Raton: Lewis Publishers).

DUNGAN, J.L., 2002, Toward a comprehensive view of uncertainty in remote sensing analysis. *Uncertainty in Remote Sensing and GIS*, **3**, pp. 25–35.

FOODY, G.M., 2002, Status of land cover classification accuracy assessment. *Remote Sensing of Environment*, **80**, pp. 185–201.

GOODCHILD, M.F. and HUNTER, G.J., 1997, A simple positional accuracy measure for linear features. *International Journal of Geographical Information Science*, **11**, pp. 299–306.

KANE, W., PETERS, D.C. and SPEIRER, R.A., 1996, Remote sensing in investigation of engineered underground structures. *Journal of Geotechnical Engineering*, **122**, pp. 674–681.

KARPUZ, C., 1982, Rock mechanics characteristics of Ankara andesites in relation to their degree of weathering. Ph.D. Thesis, METU Mining Engineering Department, Ankara, Turkey, p. 157.

KOIKE, K., NAGANO, S. and OHMI, M., 1995, Lineament analysis of satellite images using a segment tracing algorithm (STA). *Computers and Geosciences*, **21**, pp. 1091–1104.

KOOPMANS, B.N., 1986, A comparative study of lineament analysis from different remote sensing imagery over areas in the Benue Valley and Jos Plateau, Nigeria. *International Journal of Remote Sensing*, **7**, pp. 1763–1771.

LEECH, D.P., TRELOAR, P.J., LUCAS, N.S. and GROCOTT, J., 2003, Landsat TM analysis of fracture patterns: a case study from the Coastal Cordillera of northern Chile. *International Journal of Remote Sensing*, **24**, pp. 3709–3726.

LOPEZ, C., 2002, An experiment on the elevation accuracy improvement of photogrammetrically derived DEM. *International Journal of Geographical Information Science*, **16**, pp. 361–375.

MAH, A., TAYLOR, G.R., LENNOX, P. and BALIA, L., 1995, Lineament analysis of Landsat Thematic Mapper images, northern territory, Australia. *Photogrammetric Engineering and Remote Sensing*, **61**, pp. 761–773.

MAJUMDAR, T.J. and BHATTACHARYA, B.B., 1988, Application of the Haar transform for extraction of linear and anomalous patterns over part of Cambay Basin, India. *International Journal of Remote Sensing*, **9**, pp. 1937–1942.

NASA Remote Sensing Tutorial web page. Available online at: http://rst.gsfc.nasa.gov/Sect2/Sect2_8.html (accessed May 2004).

NOVAK, I.D. and SOULAKELLIS, N., 2000, Identifying geomorphic features using Landsat-5/TM data processing techniques on Lesvos, Greece. *Geomorphology*, **34**, pp. 101–109.

PCI Geomatica 8.2 Online User's Manual, 2001, Available online at: http://www.pcigeomatics.com/services/support_center/tutorials/tutorials.php (accessed May 2004).

SERRA, P., PONS, X. and SAURI, D., 2003, Post-classification change detection with data from different sensors: some accuracy considerations. *International Journal of Remote Sensing*, **24**, pp. 3311–3340.

SÜZEN, M.L. and TOPRAK, V., 1998, Filtering of satellite images in geological lineament analyses: an application to a fault zone in central Turkey. *International Journal of Remote Sensing*, **19**, pp. 1101–1114.

VANDERBRUG, G.J., 1976, Line detection in satellite imagery. *IEEE Transactions on Geoscience and Electronics*, **GE-14**, pp. 37–44.

WANG, J. and HOWARTH, P.J., 1990, Use of the Hough transform in automated lineament detection. *IEEE Transactions on Geoscience and Remote Sensing*, **28**, pp. 561–566.

WANG, L., SOUSA, W.P. and GONG, P., 2004, Integration of object-based and pixel-based classification for mapping mangroves with Ikonos imagery. *International Journal of Remote Sensing*, **25**, pp. 5655–5668.